IEEE Access
Multidisciplinary | Rapid Review | Open Access Journal

Received July 7, 2018, accepted August 14, 2018, date of publication September 3, 2018, date of current version September 28, 2018.

Digital Object Identifier 10.1109/ACCESS.2018.2868177

Identification of a Nonlinear Wheel/Rail Adhesion Model for Heavy-Duty Locomotives

JING HE[1], GUANGWEI LIU[2], JIANHUA LIU[1], CHANGFAN ZHANG[1], AND XIANG CHENG[3]

[1]College of Electrical and Information Engineering, Hunan University of Technology, Zhuzhou 412007, China
[2]Zhejiang Lancoo Corporation, Ltd., Jiaxing 314001, China
[3]CRRC Zhuzhou Electric Corporation, Ltd., Zhuzhou 412007, China

Corresponding author: Changfan Zhang (zhangchangfan@263.net)

This work was supported in part by the Natural Science Foundation of China under Grant 61773159 and Grant 61473117, in part by the Hunan Provincial Natural Science Foundation of China under Grant 2017JJ4031 and Grant 2018JJ2093, and in part by the Key Laboratory for Electric Drive Control and Intelligent Equipment of Hunan Province under Grant 2016TP1018.

ABSTRACT The optimal wheel/rail adhesion of heavy-duty locomotives under traction must be determined given that suboptimal wheel/rail adhesion may result in low creep utilization, skidding, and idling. Here, we present an algorithm for the online identification of adhesion parameters. The algorithm is used for the online parameter estimation of the nonlinear wheel/rail adhesion model. The factors that influence the wheel/rail adhesion–slip ratio relationship are analyzed and described using Burckhardt's nonlinear model. Then, an identification model is established to obtain the corresponding likelihood function within the framework of parameter identification based on maximum likelihood. Given the nonlinearity of the problem, a modified differential evolution algorithm is used for the parameter estimation of the identification model to obtain an algorithm for the online estimation of the nonlinear adhesion model. Finally, numerical simulation experiments are conducted under different conditions. Experimental results show that the proposed algorithm can address the nonlinearity of the model and the uncertainty of the rail surface environment.

INDEX TERMS Advanced modeling, differential evolution, heavy-duty locomotive, method of maximum likelihood, nonlinear identification.

I. INTRODUCTION

In heavy-duty locomotives, the requirements of adhesive utilization, anti-idling, and ramp passing are becoming increasingly stricter with increased axle load and train formation [1] . Thus, the locomotive must meet the actual needs of longitudinal traction and provide it steadily [2]. Therefore, the effective estimation of the wheel/rail adhesion performance parameters provides a basis for the control and optimization of the longitudinal traction, and can better ensure the safe operation and smooth passing of the locomotive [3].

The longitudinal traction of the heavy-duty locomotive must be achieved by the adhesion resulted from the wheel movement relative to the rail. Accordingly, when the locomotive is running, the linear speed of the wheel-set is greater than that of the locomotive, and the speed difference is the so-called creep speed. A nonlinear relationship exists between the creep speed and the adhesion, which is described as the characteristic curve of the adhesion. On this basis, the adhesion performance parameters under the current condition for the wheel and rail such as the maximum adhesion coefficient and the optimal creep point are known. As regards some of the existing estimation methods for the adhesion performance parameters, in literature [4] the recursive least square is adopted for identification of the wheel/rail adhesion model. The algorithm is adaptive to variations in the model parameters but does not duly consider perturbations introduced in the differential algorithm. In literature [5], [6], the fuzzy algorithm is used for quickly identifying traffic. However, it only considers variations in the adhesion with the third medium, with incomplete estimates on the model. In literature [7], by presetting several types of models, the current rail surface type is identified online. The algorithm is real-time and accurate. However, given that its accuracy depends on the preset model, different preset models must be applied to different locomotives. Thus, the applications of the algorithm are limited.

The wheel/rail adhesion behavior of the locomotive is part of a complex process that is subject to the axle load of the locomotive, the third medium, ambient temperature, humidity, and so on; the behavior is time-varying and nonlin-

ear [8]–[10]. For example, when the dry third medium turns into water, the adhesion coefficient will drop by 40%. When the ambient humidity rises from 20% to 100%, the adhesion coefficient will decrease by approximately 17% [11]. Therefore, the identification of the wheel/rail adhesion model for the locomotive must satisfy the nonlinear and time-varying requirements.

Several literatures [12]–[14] have proposed parameter identification methods based on project mapping, model error function and attenuation memory filter. Maximum likelihood estimation (MLE) is a widely applied algorithm for parameter estimation and indicates excellent statistical characteristics such as consistency and progressiveness [15]. The MLE algorithm constructs a likelihood function using the system model and the observed data and estimates unknown model parameters by solving the extremum of this likelihood function [16]. Accurate parameter estimation also provides a basis for control [17]. Thus, the MLE method is used to identify the adhesion model online.

The main contribution of this work is as follows. An algorithm for the identification of the adhesion model for heavy-duty locomotives is constructed under MLE by considering the nonlinear and time-varying adhesion–slip ratio relationship of locomotives. A discrete adhesion–critical model, which provides the likelihood function under MLE and uses a modified differential evolution algorithm for problem solution, is established by analyzing the adhesion behavior of locomotives. We introduce the modified variation factor to improve computational speed and sensitivity to environmental changes to enable adaptation to the unpredictable external environmental changes of the locomotive.

This paper is organized as follows. The factors that affect the adhesion performance of the locomotive are introduced in Section 2. An analysis of the wheel/rail adhesion model is presented in Section 3. The proposed identification algorithm of the nonlinear wheel/rail adhesion model for heavy-duty locomotives is discussed in Section 4. The verification of the effectiveness of the proposed MLE algorithm through simulations is discussed in section 5. The conclusion is provided in Section 6.

II. SYSTEM DESCRIPTION

The longitudinal traction of locomotives is generated by the creep between the wheels of locomotives. When the motor torque acts and drives the wheel-sets to roll, the rail segment before the contact zone is stretched as the wheel-set is compressed and that behind the contact zone behaves in the opposite manner. Microscopically, the contact zone indicates the slip ratio with the following macroperformance: When the locomotive is driven forward, the linear speed of the wheel-set is higher than the speed of the locomotive body. The speed difference is called creep speed v_s, which is expressed as follows: [18]

$$v_s = rw - v \tag{1}$$

where r represents the wheel-set radius, w represents the wheel-set angular velocity, and v represents the locomotive speed. The slip ratio λ is further defined as: [19]

$$\lambda = \frac{rw - v}{v} \tag{2}$$

In discussions about adhesion control, the adhesion coefficient μ is defined as:

$$\mu = \frac{f_{ad}}{Mg} \tag{3}$$

Where f_{ad} represents locomotive adhesion, M represents the axel traction effort, and g represents acceleration due to gravity.

Creep motion is a power source for locomotive traction and braking. The adhesion provided by the wheel/rail contact patch is divided into longitudinal, horizontal, and spin slip ratio [20]. The longitudinal slip ratio is a concern because of its dominance in traction or braking [21].

The relationship between creep speed and adhesion in the longitudinal slip ratio can be described by the characteristic curve of adhesion. The ideal characteristic adhesion curve is a smooth unimodal curve. However, the measured characteristic curve of adhesion tends to exhibit a certain width because of the uncontrollable external environment and the self-coupling and nonlinearity of locomotives.

Some studies indicate that because the locomotive is running in an open environment, the third medium, ambient temperature, air humidity and so on significantly affect the wheel/rail adhesion performance [10], [22]. Among such factors, the third medium is the most influential. For example, the adhesion coefficient with the aqueous medium drops by 40% compared with that with the dry medium [11]. Aside from the third medium, ambient temperature and air humidity affect the adhesion in a continuous time-varying manner, and the adhesion changes slowly and continuously as these quantities vary. For example, studies have shown that when the ambient humidity rises from 20% to 100%, the adhesion coefficient will drop by approximately 17% [11].

Actual adhesion performance can be effectively characterized by some creep models that are based on the creep mechanism. Most of these models are based on rolling contact theory and are highly consistent with actual adhesion performance. However, these models cannot be applied to the optimal control of traction and braking because of the introduction of some immeasurable and nonconstant quantities, such as creep patch size and friction factor.

Given the difficulties encountered by mechanistic models, empirical models fitted with measured data are generally adopted in the traction control of locomotives. These empirical models are simpler than mechanistic models and indicate the improved goodness of fit. Thus, they are widely used in controlling traction and braking.

Regardless of the type of adhesion model, the described adhesion characteristic curve is generally uni-modal. Considering this feature, in the literature, researchers considered maintaining the creep speed close to the point at which the

TABLE 1. Parameters of burckhardt's model [19], [31], [32].

Rail surface conditions	c_1	c_2	c_3
Dry	0.8287	45.45	0.4
Common	0.32	25	0.1
Wet	0.165	15	0.1

derivative thereof is less than zero, thereby attaining the maximum adhesion [23], [24]. This method can avoid obtaining adhesion performance parameters. However, such methods with differential operators or complex observers introduced are sensitive to interference and indicate certain limitations in practice.

If the wheel/rail adhesion model parameters of the locomotive are identifiable in real-time, the adhesion performance parameters under the current rail surface condition will be obtained. If differential operations are introduced in the traction and braking control of the locomotive, the locomotive is kept close to the optimal creep point, thereby increasing the adhesion utilization rate of the locomotive [25]–[27]. The key to such control methods is the real-time acquisition of adhesion performance parameters such as maximum adhesion coefficient and optimal creep point. We assume that the wheel/rail adhesion model is $\mu = f(\lambda, \boldsymbol{\theta})$, where $\boldsymbol{\theta}$ represents the model parameters. Via real-time solutions to the parameter $\boldsymbol{\theta}$, model parameters such as maximum adhesion coefficient and optimal creep point are indirectly obtained, thereby improving the passing of the locomotive and ensuring braking safety [28].

III. WHEEL/RAIL ADHESION MODEL

Based on the nonlinear magic formula tire model proposed by Pacejka, Burckhardt obtained the corresponding nonlinear model, which was coined Burckhardt's model, via theoretical deformation and simulation analysis: [29]

$$u(\lambda) = \left[c_1\left(1 - e^{-c_2\lambda}\right) - c_3\lambda\right] \cdot e^{-c_4\lambda V} \cdot \left(1 - c_5 F_Z^2\right) \quad (4)$$

In Equation (4), c_1, c_2, c_3, c_4, c_5 represents the model parameter, and λ represents the slip ratio. Given that the product of the latter two items of the model $e^{-c_4\lambda V} \cdot \left(1 - c_5 F_Z^2\right)$ is close to 1, they are generally ignored in studies on the adhesion. Thus, Burckhardt's model tends to use the following form: [30]

$$u(\lambda) = \left[c_1\left(1 - e^{-c_2\lambda}\right) - c_3\lambda\right] \quad (5)$$

The model in Equation (5) has been applied in locomotive adhesion control [31]. A control method based on the Burckhardt model has been proposed [19].

The typical model parameters are as follows:

In Burckhardt's model, $\mu(\lambda)$ represents the adhesion coefficient with λ as a variable, and c_1, c_2, c_3 represents the rail surface parameter. As for the identification, the parameters

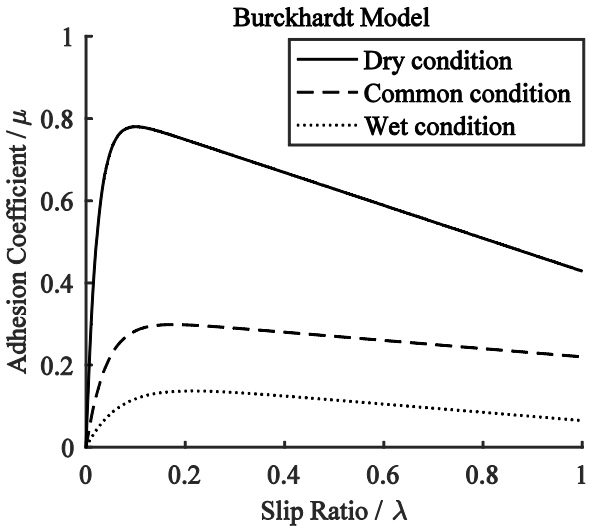

FIGURE 1. Characteristic curve of adhesion in Burckhardt's model.

to be estimated are c_1, c_2, c_3, which are denoted as $\boldsymbol{\theta} = [c_1, c_2, c_3]$. Through simple derivation, the optimal creep point that is pertinent to the adhesion control, namely the maximum adhesion coefficient $\mu_m(\lambda_m)$ and the corresponding slip ratio λ_m, can be calculated as follows:

$$\mu_m(\lambda_m) = c_1 - \frac{c_3}{c_2}\left(1 + \log\frac{c_1 c_2}{c_3}\right), \quad \lambda_m = \frac{1}{c_2}\log\frac{c_1 c_2}{c_3} \quad (6)$$

Based on Equation (6), the location of the optimal creep point is determined by c_1, c_2, c_3.

Burckhardt's model has high accuracy and few parameters. It can meet the requirements of real-time and accurate online identification provided that its nonlinear characteristics are overcome.

In summary, model parameters c_1, c_2, c_3, which are determined through online identification, can provide a remarkable basis for the control and optimization of wheel/rail adhesion.

IV. IDENTIFICATION ALGORITHM

A. SETTING THE LIKELIHOOD FUNCTION

Here, the parameter to be estimated $\boldsymbol{\theta} = [c_1, c_2, c_3]$ is solved by establishing the MLE framework. In the maximum likelihood method, we construct a likelihood function that relates to the measured data and the unknown parameters, and we obtain the parameter identification value of the model by maximizing this likelihood function.

In Equation (5), μ represent the adhesion coefficients, λ represents the slip ratio, and c_1, c_2, c_3 represents the coefficient to be identified. By outputting $\boldsymbol{z}(k) = \boldsymbol{\mu}(k)$, the data vector is $\boldsymbol{h}(k) = \boldsymbol{\lambda}(k)$, and the parameter to be identified is $\boldsymbol{\theta}(k) = [\boldsymbol{c_1}(k), \boldsymbol{c_2}(k), \boldsymbol{c_3}(k)]$. k is the sampling point. Considering the noise $\boldsymbol{n}(k) \sim \boldsymbol{N}(0, 0.01)$, the identification

model is established below:

$$z(k) = \sum_{i=1}^{N} \theta_i \cdot \boldsymbol{h}_i(k) + \boldsymbol{n}(k) = c_1 - c_1 \cdot e^{-c_2 \cdot \boldsymbol{h}(k)} - c_3 \cdot \boldsymbol{h}(k) + \boldsymbol{n}(k) \quad (7)$$

The innovation (i.e., the output prediction error equation) is

$$\tilde{z}(k) = z(k) - \hat{z}(k) = z(k) - \boldsymbol{h}^T(k)\hat{\boldsymbol{\theta}}(k-1) \quad (8)$$

Under the maximum likelihood framework, the maximum log likelihood function is obtained by Equation (7):

$$L(\boldsymbol{Z}_L|\boldsymbol{H}_{L-1}, \theta) = \ln P(Z_L|\boldsymbol{H}_{L-1}, \boldsymbol{\theta}) = c - \frac{L}{2} \cdot \ln 2\pi - \frac{1}{2 \cdot \sigma^2} \cdot \sum_{k=1}^{L} \boldsymbol{n}^2(k) \quad (9)$$

Based on the principle of maximum likelihood identification, the parameter to be identified $\boldsymbol{\theta}(k) = [\boldsymbol{c_1}(k), \boldsymbol{c_2}(k), \boldsymbol{c_3}(k)]$ is the value that facilitates a maximal logarithmic likelihood function; that is

$$\hat{\boldsymbol{\theta}} = \arg\max_{\theta} L(\boldsymbol{Z}_L|\boldsymbol{H}_{L-1}, \boldsymbol{\theta}) \quad (10)$$

Based on Equation (9), the following minimum value is taken after being divided by the constant term, thereby obtaining the maximum value of Equation (10):

$$\sum_{k=1}^{L} \boldsymbol{n^2}(k) \quad (11)$$

We introduce the identification model as Equation (8) into Equation (11):

$$\sum_{k=1}^{L} \boldsymbol{n}^2(k) = \sum_{k=1}^{L} \left(z_k - c_1 + c_1 \cdot e^{-c_2 \cdot \boldsymbol{h}(k)} + c_3 \cdot \boldsymbol{h}_k\right)^2 \quad (12)$$

The objective function is

$$\boldsymbol{J}(\theta) = \sum_{k=1}^{L} \left(z_k - c_1 + c_1 \cdot e^{-c_2 \cdot \boldsymbol{h}(k)} + c_3 \cdot \boldsymbol{h}_k\right)^2 \quad (13)$$

Based on Equation (13), the parameter to be identified $\boldsymbol{\theta}(k)$ is the value that facilitates a minimal logarithmic objective function; that is

$$\hat{\boldsymbol{\theta}} = \arg\max_{\theta} J(\theta) \quad (14)$$

In addition, since the derivation process above are maximum-likelihood based, they have associated known and asymptotically optimal statistical properties. The convergence and reliability of the algorithm are shown in the following expressions

$$\hat{\boldsymbol{\theta}} \xrightarrow[L\to\infty]{a.s.} \boldsymbol{\theta}_0 \quad (15)$$

In Equation (15), $\boldsymbol{\theta}_0$ represents the true value of model parameters.

Given that the objective function is a nonlinear equation, the general method is not applicable, and the modified differential evolution is adopted to solve the extremum. The identification framework is below.

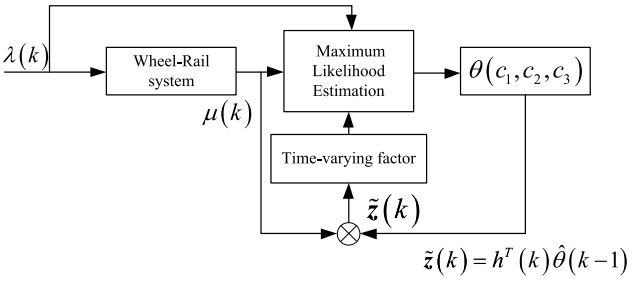

FIGURE 2. Identification framework.

B. MODIFIED DIFFERENTIAL EVOLUTION ALGORITHM

The parameters are designed for the differential evolution algorithm below.

The differential evolution algorithm is modified given that the parametric variation form of the locomotive in the actual operation is characterized by a jump that indicates time-varying characteristics. This modification improves the speed and accuracy of the algorithm.

Step 1: For the generation of the initial population, the algorithm is converted into the form of $\hat{\boldsymbol{\theta}}(k-1)$ + bell curve.

The selection of the initial value for the common differential evolution algorithm is at random in the entire value range. However, considering the actual operating conditions of the locomotive, when the locomotive is steadily running with the external environment remaining unchanged, the wheel/rail adhesion-creep is relatively stable. In that case, the parameters are slowly time-varying. To increase the convergence rate for the differential evolution algorithm, the initial population generated for the differential evolution algorithm is designed as follows:

$$x_{ij} = \boldsymbol{\theta}(k-1) + \boldsymbol{N}(0, \sigma) \quad (16)$$

Step 2: Modified variation factor

The size of the variation factor determines the diversity of the population. When the rail surface environment does not jump; that is, the innovation equation does not change too much, the variation factor should be smaller. Furthermore, by accelerating the convergence of the algorithm, unnecessary calculations may be avoided. When the innovation equation changes significantly, the variation factor should be greater, thereby ensuring that algorithm jumps faster out of local extremum. Aided by the logistic function, the time-varying variation factor is designed as follows:

$$\boldsymbol{F}(k) = 0.3 + \frac{0.8}{1 + e^{-10 \cdot |\tilde{z}(k)| + 2}} \quad (17)$$

C. FLOWCHART OF THE ALGORITHM

Figure 3 describes the flow of the algorithm. First, the parameters of the differential evolution algorithm are initialized in accordance with Table 2. The initialization group is generated in accordance with Equation (16) and proceeds in the loop

TABLE 2. Differential algorithm parameters.

Quantity	Value
Population size:	20
Number of parameters:	3
Variance factor:	$F(k)$
Cross factor:	0.6
Max number of iterations:	300
Parameter search range:	[0.1 10 0.05]-[1 50 0.5]

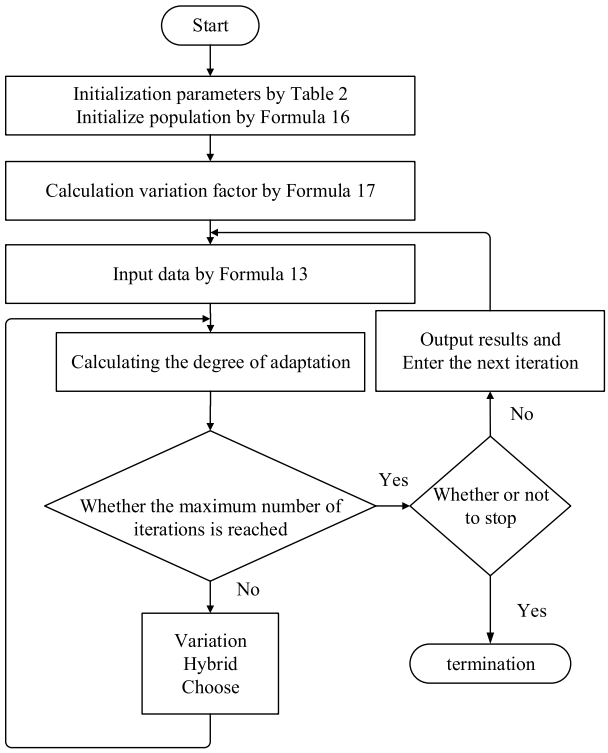

FIGURE 3. Algorithm flowchart.

to find the extremes. Finally, the online estimation of the parameters is achieved.

V. SIMULATION ANALYSIS

We design three simulation experiments to verify the validity of the algorithm.

In Experiment 1, we simulate the identification results of the model for a locomotive that runs on a single rail surface. The situation in which the rail environment is switched is considered.

In Experiment 2, we determine whether the algorithm can effectively adapt to changes in the rail surface and track the real-time changes in the rail surface in a timely manner.

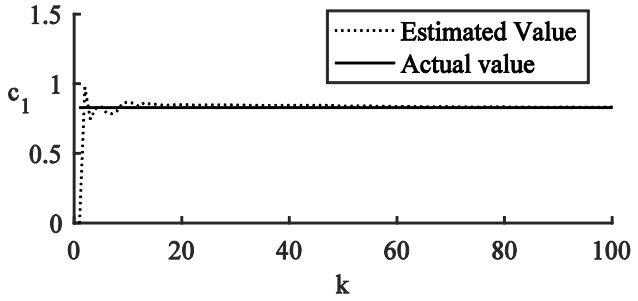

FIGURE 4. Identification results of c_1.

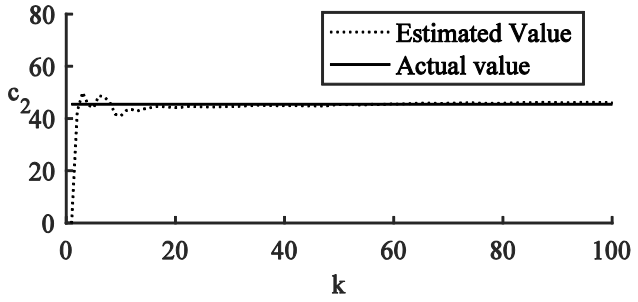

FIGURE 5. Identification results of c_2.

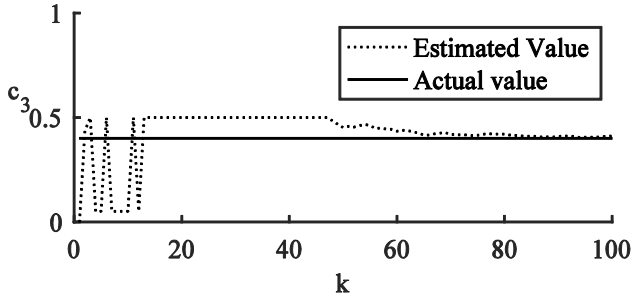

FIGURE 6. Identification results of c_3.

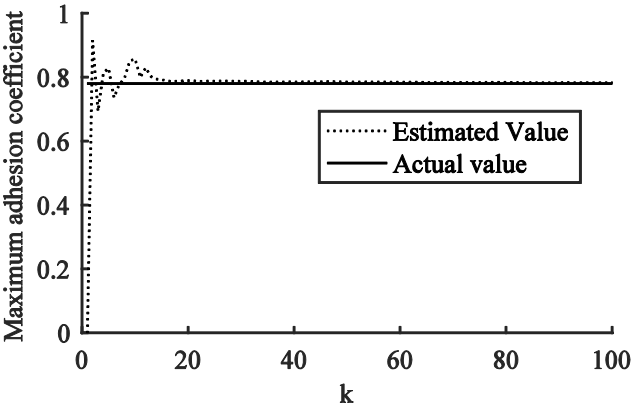

FIGURE 7. Identification results of the maximum adhesion coefficient.

In Experiment 3, we perform a control experiment to investigate the effects of the modified time-varying differential evolution algorithm.

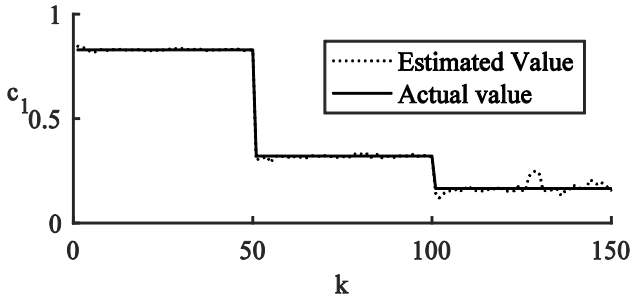

FIGURE 8. Identification results of c_1.

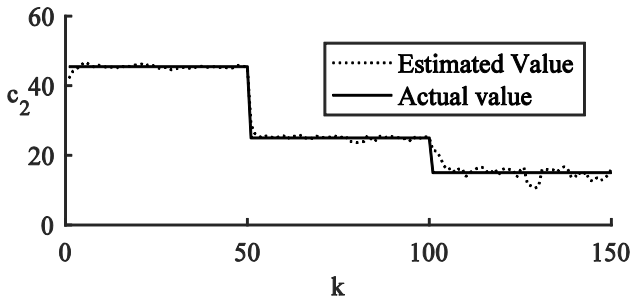

FIGURE 9. Identification results of c_2.

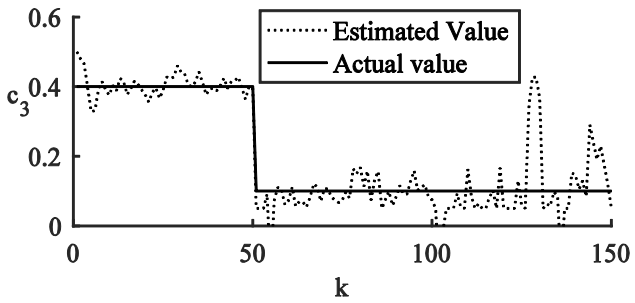

FIGURE 10. Identification results of c_3.

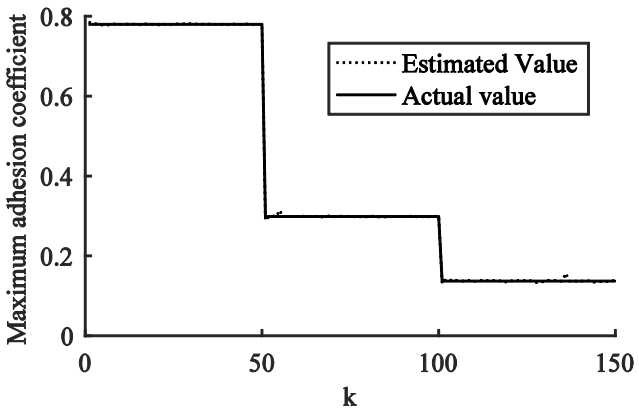

FIGURE 11. Identification results of the maximum adhesion coefficient.

Experiment 1: We conduct the parameter identification of sequence processing on the single rail surface and estimate the most important adhesion performance parameter, namely,

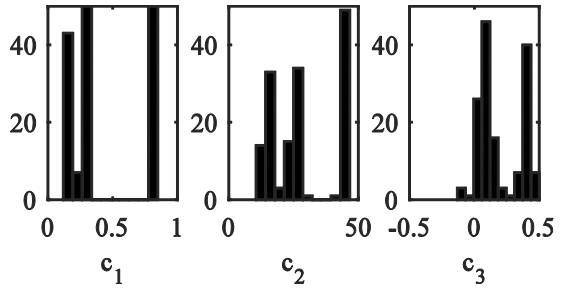

FIGURE 12. Histogram of the maximum adhesion coefficient.

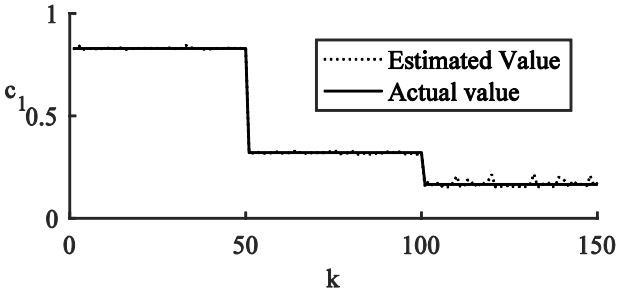

FIGURE 13. Identification results of c_1.

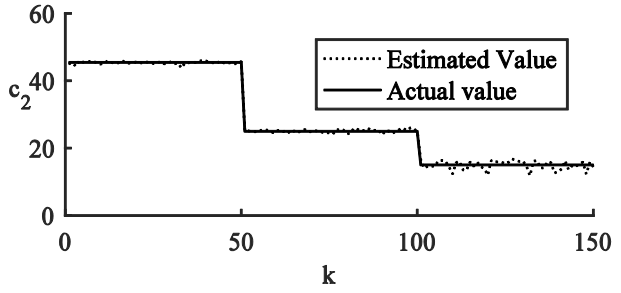

FIGURE 14. Identification results of c_2.

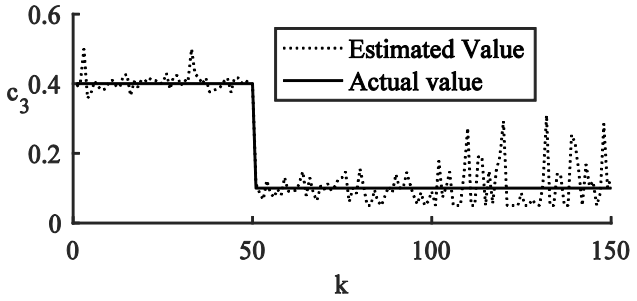

FIGURE 15. Identification results of c_3.

the point of peak adhesion. Input signals mainly consider the actual train driving conditions in the creeping zone, and only a small part of the data points indicate idling. Thus, the data designed for the simulation experiments only contain the relevant data with the slip ratio within the range of [0, 0.5].

By setting the noise to $\boldsymbol{v}(k) \sim \boldsymbol{N}(0, 0.01)$, and the initial value of the estimation algorithm is randomly generated

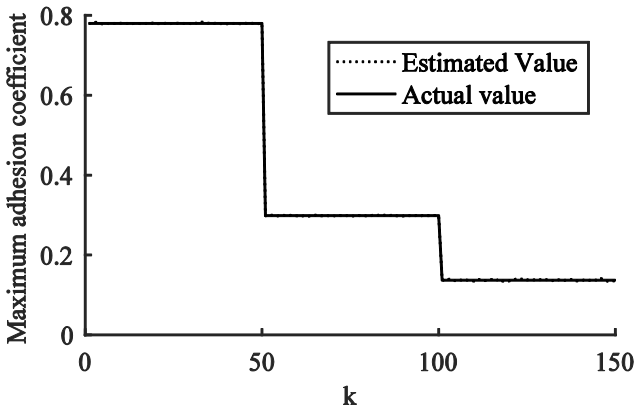

FIGURE 16. Identification results of the maximum adhesion coefficient.

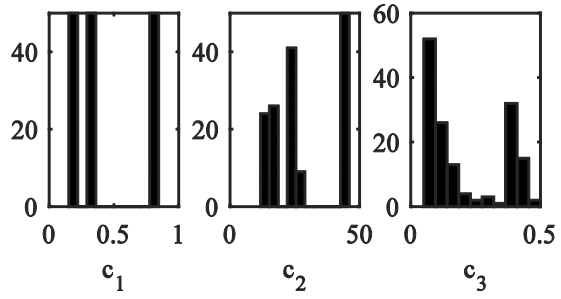

FIGURE 17. Histogram of the maximum adhesion coefficient.

within the parameter search range. The experimental results are below.

The simulation results indicate that parameter c_1, c_2 has already converged to a true value at the slip ratio of approximately 0.1. The parameter with the largest error c_3 begins to converge at a slip ratio of approximately 0.4, and the corresponding maximum adhesion coefficient converges to near a true value. This result suggests that the algorithm can converge within an acceptable range.

Experiment 2: In actual locomotive operation, the external environment may suddenly change, and parameters are slowly changing. Thus, we consider the validity of the algorithm in the case of a sudden change in the rail surface. Each data block contains 500 data points after processing. The data used in the simulation experiment are also incomplete and only contain data with a slip ratio within the range of [0, 0.2].

By setting the noise to $\boldsymbol{v}(k) \sim \boldsymbol{N}(0, 0.01)$, and the initial value of the estimation algorithm to $[c_1(0) = 0.5, c_2(0) = 30, c_3(0) = 0.08]$, we conduct a Monte Carlo experiment to verify the adaptability of the estimation algorithm in practice. The experiment results are as follows:

The simulation results indicate that after modification through block processing, the effects of the algorithm have improved. In particular, the effect of the algorithm on rail surface adhesion coefficient, which is of particular interest in adhesion control, has considerably improved. The origin of the maximum error from parameter c_3 indicates relatively high volatility.

Experiment 3: In the control experiment, we add the modified experiment results to illustrate the validity of the modified differential algorithm. Except for the improvements mentioned in 4.2, nearly all the parameters are the same as those in Experiment 2. The innovation equation for the summation in the block processing is substituted for the original innovation equation. The experimental results are as follows:

We compare Experiments 2 and 3 where $k = 50$ and $k = 100$, respectively. That is, the rail surface environment presents a sudden change. In this situation, we find that the volatility of the estimation results is greatly reduced given the two improvements in the differential algorithm. When the surface environment changes suddenly, the modified algorithm allows for the rapid tracking of parameter transitions. The histogram also indicates that the estimation results are concentrated. Ideally, the solution of the algorithm is accelerated by improving the variation factor. However, the maximum number of iterations is limited because the calculation is finite. Therefore, the modified variation factor can improve accuracy and tracking speed with limited calculation.

VI. CONCLUSIONS

The identification of the proposed nonlinear wheel/rail adhesion model for heavy-duty locomotives is suitable for the parameter estimation of the relationship between the wheel-set and the rail in a nonlinear, time-varying, and noisy environment with incomplete data. An algorithm for parameter identification for the wheel/rail adhesion model based on Burckhardt's nonlinear model is obtained through maximum likelihood. We obtain an algorithm for parameter estimation by introducing a modified differential evolution algorithm to cope with the nonlinear difficulties encountered by the model and to solve the corresponding likelihood function. The introduction of the time-varying variation factor accelerates the solution of the algorithm and increases the adaptability of the algorithm to the environment. The results of simulation experiments illustrate that the estimation algorithm effectively tracks changes in the wheel/rail of locomotives and compensates for missing locomotive data.

Future research based on this work may focus on the tracking speed of the optimization algorithm. A gradient descent algorithm with high robustness may be applied as an alternative to the differential evolution algorithm used in this work.

REFERENCES

[1] X. Wang, T. Tang, and H. He, "Optimal control of heavy haul train based on approximate dynamic programming," *Adv. Mech. Eng.*, vol. 9, no. 4, pp. 1–15, 2017.
[2] M. Spiryagin, P. Wolfs, C. Cole, S. Stichel, M. Berg, and P. C. Manfred, "Influence of AC system design on the realisation of tractive efforts by high adhesion locomotives," *Vehicle Syst. Dyn.*, vol. 55, no. 8, pp. 1241–1264, 2017.
[3] C. Uyulan, M. Gokasan, and S. Bogosyan, "Comparison of the re-adhesion control strategies in high-speed train," *Inst. Mech. Eng., I, J. Syst. Control Eng.*, vol. 232, no. 1, pp. 92–105, 2017.

[4] Y. F. Li, X. Y. Feng, and R. K. Liu, "Maximum adhesion control of railway based on sliding mode control system," *Adv. Mater. Res.*, vols. 383–390, pp. 5242–5249, Nov. 2011.

[5] H. Dahmani, M. Chadli, A. Rabhi, and A. El Hajjaji, "Road curvature estimation for vehicle lane departure detection using a robust Takagi–Sugeno fuzzy observer," *Vehicle Syst. Dyn.*, vol. 51, no. 5, pp. 581–599, 2013.

[6] Y. Tian, W. Daniel, S. Liu, and P. A. Meehan, "Fuzzy logic creep control for a 2D locomotive dynamic model under transient wheel-rail contact conditions," *WIT Trans. Built Environ.*, vol. 135, pp. 885–896, Jun. 2014.

[7] M. Spiryagin, C. Cole, and Y. Q. Sun, "Adhesion estimation and its implementation for traction control of locomotives," *Int. J. Rail Transp.*, vol. 2, no. 3, pp. 187–204, 2014.

[8] H. Chen and H. Tanimoto, "Experimental observation of temperature and surface roughness effects on wheel/rail adhesion in wet conditions," *Int. J. Rail Transp.*, vol. 6, no. 2, pp. 101–112, 2018.

[9] L. Diao, L. Zhao, Z. Jin, L. Wang, and S. M. Sharkh, "Taking traction control to task: High-adhesion-point tracking based on a disturbance observer in railway vehicles," *IEEE Ind. Electron. Mag.*, vol. 11, no. 1, pp. 51–62, Mar. 2017.

[10] I. A. Radionov and A. S. Mushenko, "The method of estimation of adhesion at 'wheel-railway' contact point," in *Proc. Int. Siberian Conf. Control Commun. (SIBCON)*, 2015, pp. 1–5.

[11] D. Smejkal, M. Omasta, and M. Hartl, "An experimental investigation of the adhesion behavior between wheel and rail under oil, water and sanding conditions," in *Modern Methods of Construction Design*. Cham, Switzerland: Springer, 2014, pp. 623–628.

[12] Q. Guo, Y. Zhang, B. Celler, and S. Su, "Backstepping control of electro-hydraulic system based on extended-state-observer with plant dynamics largely unknown," *IEEE Trans. Ind. Electron.*, vol. 63, no. 11, pp. 6909–6920, Nov. 2016.

[13] Q. Guo, P. Sun, J. M. Yin, T. Yu, and D. Jiang, "Parametric adaptive estimation and backstepping control of electro-hydraulic actuator with decayed memory filter," *ISA Trans.*, vol. 62, pp. 202–214, May 2016.

[14] Q. Guo, J. Yin, T. Yu, and D. Jiang, "Saturated adaptive control of an electrohydraulic actuator with parametric uncertainty and load disturbance," *IEEE Trans. Ind. Electron.*, vol. 64, no. 10, pp. 7930–7941, Oct. 2017.

[15] K. Dolinský and S. Čelikovský, "Application of the method of maximum likelihood to identification of bipedal walking robots," *IEEE Trans. Control Syst. Technol.*, vol. 26, no. 4, pp. 1500–1507, Jul. 2017.

[16] C. Han and P. C. B. Phillips, "First difference maximum likelihood and dynamic panel estimation," *J. Econometrics*, vol. 175, no. 1, pp. 35–45, 2013.

[17] C. Li, Z. Chen, and B. Yao, "Adaptive robust synchronization control of a dual-linear-motor-driven gantry with rotational dynamics and accurate online parameter estimation," *IEEE Trans. Ind. Inform.*, vol. 14, no. 7, pp. 3013–3022, Jul. 2017.

[18] S. Sadr, D. A. Khaburi, and M. Namazi, "A comprehensive model for adhesion control system of wheel and rail," *J. Oper. Automat. Power Eng.*, vol. 5, no. 1, pp. 43–50, 2017.

[19] Y. Chen, H. Dong, J. Lü, X. Sun, and L. Guo, "A super-twisting-like algorithm and its application to train operation control with optimal utilization of adhesion force," *IEEE Trans. Intell. Transp. Syst.*, vol. 17, no. 11, pp. 3035–3044, Nov. 2016.

[20] Z. A. Soomro, "Adhesion detection analysis by modeling rail wheel set dynamics under the assumption of constant creep coefficient," *J. Mechatron., Elect. Power, Veh. Technol.*, vol. 5, no. 2, pp. 99–106, 2014.

[21] Y. Tian, S. Liu, W. J. T. Daniel, and P. A. Meehan, "Investigation of the impact of locomotive creep control on wear under changing contact conditions," *Vehicle Syst. Dyn.*, vol. 53, no. 5, pp. 692–709, 2015.

[22] K. Ishizaka, S. R. Lewis, and R. Lewis, "The low adhesion problem due to leaf contamination in the wheel/rail contact: Bonding and low adhesion mechanisms," *Wear*, vols. 378–379, pp. 183–197, May 2017.

[23] M. Yamashita and T. Soeda, "Anti-slip re-adhesion control method for increasing the tractive force of locomotives through the early detection of wheel slip convergence," in *Proc. 17th Eur. Conf. Power Electron. Appl. (EPE ECCE-Europe)*, 2015, pp. 1–10.

[24] K. Xu, G. Xu, and C. Zheng, "Novel determination of wheel-rail adhesion stability for electric locomotives," *Int. J. Precision Eng. Manuf.*, vol. 16, no. 4, pp. 653–660, 2015.

[25] S. Sadr, D. A. Khaburi, M. Namazi, A. Shiri, and D. E. Moghadam, "Modeling of wheel and rail slip and demonstration of the benefit of maximum adhesion control in train propulsion system," in *Proc. IEEE 23rd Int. Symp. Ind. Electron. (ISIE)*, Jun. 2014, pp. 847–852.

[26] Ö. Ararat and M. T. Söylemez, "Robust velocity estimation for railway vehicles," *IFAC-PapersOnLine*, vol. 50, no. 1, pp. 5961–5966, 2017.

[27] Q. Peng, J. Liu, Z. Huang, W. Liu, and H. Li, "Sliding model control based on estimation of optimal slip ratio for railway wheel slide protection using extremum seeking," in *Proc. ECCE*, 2016, pp. 1–6.

[28] Z. A. Soomro, "Computation of Slip analysis to detect adhesion for protection of rail vehicle and derailment," *J. Appl. Comput. Mech.*, vol. 1, no. 3, pp. 145–151, 2015.

[29] Ç. Uyulan and M. Gokasan, "Modeling, simulation and re-adhesion control of an induction motor–based railway electric traction system," *Inst. Mech. Eng., I, J. Syst. Control Eng.*, vol. 232, no. 1, pp. 3–11, 2017.

[30] C. Uyulan, M. Gokasan, and S. Bogosyan, "Modeling, simulation and slip control of a railway vehicle integrated with traction power supply," *Cogent Eng.*, vol. 4, no. 1, 2017, Art. no. 1312680.

[31] M. Zhou, Y. Song, W. Cai, L. Fan, and F. Liu, "Neuro-adaptive anti-slip brake control of high-speed trains," in *Proc. Control Conf.*, 2013, pp. 291–296.

[32] H. Chen, W. Cai, and Y. Song, "Wheel skid prediction and antiskid control of high speed trains," in *Proc. IEEE Int. Conf. Intell. Transp. Syst.*, Oct. 2014, pp. 1209–1214.

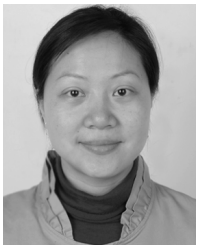

JING HE received the M.S. degree in computer engineering from the Central South University of Forestry and Technology, Changsha, China, in 2002, and the Ph.D. degree in mechatronics engineering from the National University of Defense Technology, Changsha, in 2009. She was a Visiting Research Fellow with the Helsinki University of Technology, Helsinki, Finland, from 2004 to 2005. She was with the University of Waterloo, Waterloo, Canada, from 2007 to 2008, and the Tokyo University of Technology, Tokyo, Japan, in 2016. She was also with the University of Alabama, Tuscaloosa, USA, in 2017. Since 1992, she has been with the College of Electrical and Information Engineering, Hunan University of Technology, Zhuzhou, China. She has been a Professor with the Hunan University of Technology since 2009. Her research interests include fault diagnosis on mechatronics machines and industrial process control.

GUANGWEI LIU received the B.Sc. degree from the Hunan Institute of Science and Technology in 2015. He is currently pursuing the M.Sc. degree with the Hunan University of Technology. His main research direction is complex systems modeling.

JIANHUA LIU received the M.S. and Ph.D. degrees in control science and engineering from Central South University, Changsha, China, in 2009 and 2013, respectively. Since 2013, he has been with the College of Traffic Engineering, Hunan University of Technology, Zhuzhou, China. His main research interests include fault diagnosis on industrial process.

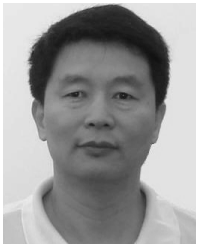

CHANGFAN ZHANG received the M.S. degree in electronics engineering from Southwest Jiaotong University, Chengdu, China, in 1989, and the Ph.D. degree in control theory and engineering from Hunan University, Changsha, China, in 2001. He was a Post-Doctoral Fellow with Central South University, Changsha, from 2001 to 2003, and a Visiting Research Fellow with the University of Waterloo, Waterloo, Canada, from 2007 to 2008. Since 1982, he has been with the College of Electrical and Information Engineering, Hunan University of Technology, Zhuzhou, China. He has been a Professor with the Hunan University of Technology since 2001. His research interests include fault diagnosis on electrical machines and industrial process control.

XIANG CHENG received the M.S. degree in electronics engineering from the Hunan University of Technology, Zhuzhou, China, in 2018. After graduation, he is currently with CRRC Zhuzhou Electric Corporation, Ltd., where he is involved in electric vehicle research and development.